Energy-Efficient Vehicular Heterogeneous Networks for Green Cities

Zhenyu Zhou, *Senior Member, IEEE*, Fei Xiong, Chen Xu, *Member, IEEE*, Yejun He, *Senior Member, IEEE*, and Shahid Mumtaz, *Senior Member, IEEE*

***Abstract*—With the evolutionary development of automobile industry, modern transportation systems cause a series of critical problems, such as increased energy consumption and air pollution. To make green cities a reality, an ever expanding and evolving vehicular heterogeneous network infrastructure is required to enable fine-granularity data collection and reliable service delivery. In this paper, we investigate how to realize energy-efficient vehicular heterogeneous networks for green cities by exploring cooperative two-hop device-to-device-based vehicle-to-vehicle (D2D–V2V) transmission. We propose a two-stage energy-efficient resource allocation algorithm. In the first stage, an auction-matching-based joint relay selection, spectrum allocation, and power control algorithm is derived, which employs an English-auction approach for matching preference updating and conflict avoidance, and optimizes the energy efficiency of two-hop D2D–V2V and cellular links simultaneously in an iterative fashion. In the second stage, a nonlinear fractional programming based power control algorithm is developed to maximize the energy efficiency of the base station. Theoretical properties in terms of convergence, stability, and complexity are analyzed. Finally, the proposed algorithm is evaluated based on real-world road topology and realistic vehicular traffic. Numerical results demonstrate that the proposed algorithm achieves superior performance in terms of energy efficiency and network coverage compared to other heuristic algorithms.**

***Index Terms*—Auction-matching, cooperative two-hop device-to-device-based vehicle-to-vehicle (D2D–V2V) transmission, energy efficiency, green city, nonlinear fractional programming.**

Manuscript received August 18, 2017; revised October 29, 2017; accepted November 16, 2017. Date of publication November 23, 2017; date of current version April 3, 2018. This work was supported in part by the National Science Foundation of China (NSFC) under Grant 61601181, in part by the Fundamental Research Funds for the Central Universities under Grant 2017MS13, in part by Beijing Natural Science Foundation under Grant 4174104, and in part by Beijing Outstanding Young Talent under Grant 2016000020124G081. Paper no. TII-17-1861. (*Corresponding author: Chen Xu.*)

Z. Zhou, F. Xiong and C. Xu are with the State Key Laboratory of Alternate Electrical Power System with Renewable Energy Sources, School of Electrical and Electronic Engineering, North China Electric Power University, Beijing 102206, China (e-mail: zhenyu_zhou@ncepu.edu.cn; fei.xiong@ncepu.edu.cn; chen.xu@ncepu.edu.cn).

Y. He is with the College of Information Engineering, Shenzhen University, Shenzhen 518060, China (e-mail: yjhe@szu.edu.cn).

S. Mumtaz is with the Institutõ de Telecomunicações, Aveiro 1049-001, Portugal (e-mail: smumtaz@av.it.pt).

Color versions of one or more of the figures in this paper are available online at http://ieeexplore.ieee.org.

Digital Object Identifier 10.1109/TII.2017.2777139

I. Introduction

A. Background and Motivation

With the evolutionary development of urbanization and automobile industry, modern transportation systems with billions of vehicles cause a series of critical problems, such as increased energy consumption, air pollution, and greenhouse gas emission [1], [2]. In the United States, the transportation sector accounts for 32% of the overall CO_2 emission, and traffic congestions cause approximate 2 billion gallons of waste fuel [3], [4]. To create future green and sustainable cities, we need an ever expanding and evolving vehicular heterogeneous network infrastructure to enable fine-granularity data collection and reliable service delivery, which is essential to the successful realization of environment-harmonic intelligent transportation systems (ITS) [5]. Among various fundamental technologies [6], vehicle-to-vehicle (V2V) communication, which supports ubiquitous information exchange and content sharing among vehicles with little or no human intervention, is a key enabler for realizing the ITS framework. It provides unprecedented opportunities for developing new green ITS applications in domains of road safety, travel efficiency, and smart energy management [7], [8].

One of the well-discussed V2V solutions is the ad-hoc-based IEEE 802.11p protocol, which operates in the 5.9-GHz ITS band and adopts the legacy carrier sense multiple access with collision avoidance (CSMA/CA) mechanism in the medium access control layer [9]. A drawback is that the contention-based CSMA/CA scheme with random backoff may result in unpredictable transmission latency when all vehicles contend to access the same available channels [10], [11]. An alterative solution is based on device-to-device (D2D) communication, which allows direct data transmission over proximate peer-to-peer links with the assistance of centralized base stations [12], [13]. Compared to the ad-hoc fashioned solutions, device-to-device-based vehicle-to-vehicle (D2D–V2V) communication can easily realize reliable service delivery and coordinated resource allocation by exploring the ubiquitous presence of base stations with global knowledge and powerful signal processing capability [10], [14].

In conventional cellular networks, communication requests of all the vehicles have to be served by the base station, which is not only energy inefficient, but also puts a heavy burden on the delay and capacity constrained backhaul links [15]. Hence, D2D–V2V communication can be applied to achieve enormous

energy efficiency improvement by effective data offloading via either single-hop or multihop transmissions. Considering the dynamic and unreliable vehicular connections caused by high mobility and sparse distribution, cooperative multihop D2D–V2V transmission will play an important role for enabling vehicles with inferior channel conditions to exchange data seamlessly [16]. In this paper, a cooperative two-hop D2D–V2V transmission mode is adopted, in which data are first forwarded by some cooperative relay in the middle and then delivered to the receiver in a hop-by-hop fashion [17]. The key research problem is how to realize energy-efficient data offloading with cooperative two-hop D2D–V2V transmission.

However, the successful realization of vehicular heterogeneous networks with cooperative D2D–V2V transmission still faces the following critical issues. First, co-channel interference caused by spectrum reusing has to be carefully managed to satisfy stringent quality of service (QoS) requirements in delay-sensitive vehicular networks [11], [18], [19]. Second, compared to the single-hop scenario, the cooperative two-hop D2D–V2V transmission mode involves a more sophisticated relay selection problem, which has to be jointly optimized with spectrum allocation and power control from an energy efficiency perspective [20]. Last but not least, performance should be evaluated in a trustworthy manner based on realistic macromobility (real-world road/street topology, traffic signs, etc.) and micromobility (acceleration/deceleration, V2V interactions, vehicle-to-road interactions, overtaking, etc.) descriptions [21].

B. State of the Art

A number of works have already studied energy-efficient resource allocation problems in conventional D2D relay networks [20], [22], [23]. A matching-based energy-efficient interference-aware resource allocation problem was developed in [20], in which the complicated joint peer discovery and relay selection problem was decomposed into two stages to reduce matching dimensionality. In [22], an energy-efficient mobile association algorithm was proposed to jointly optimize mode switching, relay selection, access point association, and power allocation. These works were mainly developed based on ideal theoretical D2D models with constant network topology and are not applicable for highly dynamic vehicular networks. The performance has not been evaluated in real-world road and street topologies with realistic vehicular traffic and mobility descriptions.

Relay-based cooperative vehicular networks have been studied in [24]–[27]. In [24], the feasibility of vehicular networks as a relay between base stations and end users was investigated. A precoded relay selection scheme was developed by exploring rich spatial diversity in V2V links. A cooperative relay broadcasting scheme was proposed in [25] to guarantee the reliability of vehicular broadcasting services in terms of packet reception and delivery rates. The relay selection problem with imperfect channel state information (CSI) was solved by using a Markov chain based channel prediction scheme. In [26], a relay localization and selection algorithm was proposed to maximize end-to-end capacity in IEEE 802.16j based vehicular networks. A highway mobility model was adopted to derive the cumulative distribution function (CDF) of capacity, and the relay selection problem was formulated as a nonlinear programming problem and solved by Lagrange dual decomposition. Vehicular data cloud services such as relay-aided intelligent parking and vehicular data mining were studied in [27], and naive Bayes and logistic regression models were developed for data mining.

Matching theory, which provides mathematically tractable solutions for matching players depending on their preferences, has been regarded as a promising technique to address resource allocation problems [28]. In [16], the authors developed a pricing-based iterative matching algorithm to maximize the total sum rate of D2D–V2V pairs. A pricing-based two-stage matching algorithm was proposed to solve the joint relay selection and resource allocation problem to improve energy efficiency (EE) performance in [20]. In [29], the authors modeled the cognitive radio networks as a matching market and derived the sufficient and necessary conditions in two different scenarios for achieving a stable matching.

However, most of the above-mentioned works were mainly developed for ad-hoc-based vehicular networks, and cannot be directly applied for D2D–V2V networks since the specific characteristics of cooperative two-hop D2D–V2V transmission have been largely neglected. Furthermore, only few works target the optimization of energy efficiency, and thus, the corresponding problem formulations are completely different from our work. Last but not least, there still lacks a unified treatment of the joint relay selection, spectrum allocation, and power control optimization problem considered in this paper from an energy efficiency perspective.

C. Contribution

We summarize the major contributions of this paper as follows.

1) We investigate how to realize energy-efficient vehicular heterogeneous networks for green cities by exploring cooperative two-hop D2D–V2V transmission. The energy efficiency maximization problem is formulated as a two-stage joint vehicular and wireless resource optimization problem. In the first stage, the vehicular relay selection, spectrum resource allocation, and transmission power control are jointly optimized to maximize the energy efficiency of two-hop D2D–V2V links and cellular links. The second stage involves a power allocation problem to optimize the energy efficiency of the base station.
2) To provide a tractable solution, we propose an auction-matching-based energy-efficient resource allocation algorithm, which employs an English-auction approach for matching preference updating and conflict avoidance, and solves the joint optimization problem in an iterative fashion. In the second stage, a nonlinear fractional programming based energy-efficient power control algorithm is proposed for the base station. In-depth analysis is also provided for theoretical properties in terms of stability, convergence, and complexity.
3) We evaluate the energy efficiency performance based on real-world road topology and realistic vehicular traffic by connecting SUMO with MATLAB through predefined in-

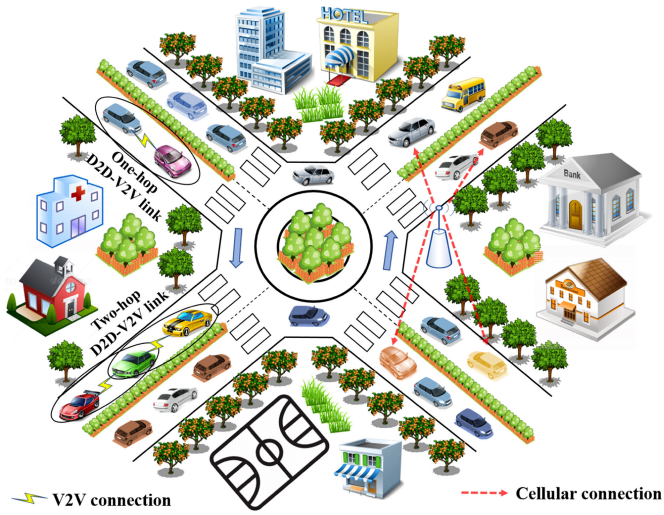

Fig. 1. Vehicular heterogeneous network with cooperative two-hop D2D–V2V transmission.

terfaces. Both macromobility and micromobility features such as road topology, traffic signs, acceleration, deceleration, overtaking, etc., are taken into consideration. The proposed algorithm is compared with several heuristic algorithms, including brute-force search, random matching without power control, and nonrelay-based matching. Numerical results demonstrate that superior performance in terms of energy efficiency and network coverage can be achieved by the proposed algorithm.

The remaining parts of this paper are organized as follows. Section II presents the system model of a vehicular heterogeneous network with cooperative two-hop D2D–V2V transmission. Problem formulation is provided in Section III. Section IV describes the proposed two-stage energy-efficient resource allocation algorithm. Performance evaluation is presented in Section V. Section VI concludes the paper and identifies future research directions.

II. System Model

In conventional cellular networks, communication requests of all the vehicles have to be served by the base station, which consumes a lot of energy and makes the cell overload problem even worse. An alternative solution is offloading the high volumes of vehicular data from cellular infrastructures to vehicular networks by utilizing D2D–V2V transmission. In particular, we focus on those D2D–V2V pairs that cannot support direct single-hop transmission due to inferior channel conditions caused by high vehicle mobility and sparse distribution. A cooperative two-hop D2D–V2V transmission mode is adopted to improve the energy efficiency of the overall heterogeneous network and the vehicular network coverage. In the following paragraphs, we introduce channel model and cooperative two-hop D2D–V2V transmission model in details.

Fig. 1 shows a vehicular heterogeneous network, which consists of a base station, K cellular user equipments (CUEs), M potential vehicular transmitters (denoted as V-TXs) and receivers (denoted as V-RXs), and N vehicular relay stations (denoted as V-RSs). The sets of M V-TXs, M V-RXs, and N V-RSs are denoted as $\mathcal{V}_{\mathrm{TX}} = \{V_1^{\mathrm{TX}}, V_2^{\mathrm{TX}}, \ldots, V_i^{\mathrm{TX}}, \ldots, V_M^{\mathrm{TX}}\}$, $\mathcal{V}_{\mathrm{RX}} = \{V_1^{\mathrm{RX}}, V_2^{\mathrm{RX}}, \ldots, V_i^{\mathrm{RX}}, \ldots, V_M^{\mathrm{RX}}\}$, and $\mathcal{V}_{\mathrm{RS}} = \{V_1^{\mathrm{RS}}, V_2^{\mathrm{RS}}, \ldots, V_n^{\mathrm{RS}}, \ldots, V_N^{\mathrm{RS}}\}$, respectively.

We assume that each CUE preoccupies one uplink orthogonal resource block, and the sets of K CUES and K resource blocks are denoted as $\mathcal{C}_V = \{C_1^V, C_2^V, \ldots, C_k^V, \ldots, C_K^V\}$ and $\mathcal{C}_{\mathrm{RB}} = \{C_1^{\mathrm{RB}}, C_2^{\mathrm{RB}}, \ldots, C_k^{\mathrm{RB}}, \ldots, C_K^{\mathrm{RB}}\}$, respectively. The uplink spectrum reusing scenario is adopted, in which each resource block can be reused simultaneously by at most one D2D–V2V transmission. In the two-hop transmission mode, assuming V-TX V_i^{TX}, V-RX V_i^{RX}, and V-RS V_n^{RS} form a cooperative D2D–V2V transmission by reusing resource block C_k^{RB} allocated to C_k^V, data are first sent from V_i^{TX} to V_n^{RS} in the first hop, and then are forwarded from V_n^{RS} to V_i^{RX} in the second hop. C_k^{RB} is reused at both the first and second hops.

In vehicular networks, it is usually infeasible to acquire real-time CSI due to fast channel variations caused by high vehicle mobility. Results in [11] and [14] have demonstrated that the mere consideration of large-scale fading effects such as path loss results in little performance degradation. By adopting similar vehicular channel models, small-scale fading effects can be neglected, and free space propagation path-loss model is incorporated for performance evaluation. It is noted that the path-loss model does not impact the solution structure of the proposed algorithm, which can be extended to more complex and practical models.

Remark 1: In this paper, we assume that the D2D–V2V peer discovery process is completed based on some existing schemes [20], [22]. However, different from peer discovery problems in conventional D2D relay networks, vehicle connection probability must be taken into consideration in D2D–V2V transmission [30], [31]. In general, it is intuitive to explore reliable and long-lasting vehicular connections for D2D–V2V link establishment. Taking TX–RX pair $(V_i^{\mathrm{TX}}, V_i^{\mathrm{RX}})$ as an example, the headway distance from V_i^{TX} to V_i^{RX} after time t is denoted as $H_i(t)$, e.g., $H_i(t) > 0$ represents that V_i^{TX} is ahead of V_i^{RX}, and $H_i(t) \leq 0$ otherwise. The specific expression of $H_i(t)$ depends on various key parameters such as the mean and variance of vehicular velocities. Denoting L as the maximum transmission distance for any one-hop D2D–V2V link, the connection time T_i between V_i^{TX} to V_i^{RX} in the two-hop transmission mode is given by

$$T_i = \{\min t \mid H_i(0) = h_{i,0}, -2L < H_i(\tau) < 2L, 0 \leq \tau \leq t\}. \tag{1}$$

Let v_i, a_i and v_m, a_m denote the mean value and variance of vehicle V_i^{TX} and V_m^{RX}, respectively. To evaluate T_i, we model the headway distance $H_i(t)$ as a Wiener process and obtain the two parameters, i.e., variance $\sigma_{i,m}^2 = a_i + a_m$ and the drift $\lambda_{i,m} = v_i - v_m$. Due to the fact that the Kolmogorov equation can describe the probability density function (PDF) of a vehicle's velocity when it is modeled as a Wiener process, the CDF of the connection time T_i is denoted as $F_i(t) = \Pr\{T_i \leq t\}$. V_i^{TX} and V_i^{RX} are allowed to form a TX–RX pair if and only if the connection probability is above certain predefined thresholds β_i, i.e, $F_i(t) \geq \beta_i$. In summary, the joint D2D–V2V mode selection

and peer discovery problem is out of the scope of this paper and will be discussed in future works.

Owing to spectrum reusing, V-TX V_i^{TX} and V-RS V_n^{RS} cause co-channel interference to the base station. V-RS V_n^{RS} (or V-RX V_i^{RX}) receives co-channel interference when CUE C_k^V transmits signal at the first hop (or at the second hop). We define $y_{k,f}$ as the hop selection variable for C_k^V, i.e., $y_{k,f}=1$ and $1-y_{k,f}=1$ represent that C_k^V operates in the first hop and second hop, respectively. The signal-to-interference-plus-noise ratio (SINR) expressions of TX–RS pair $(V_i^{\mathrm{TX}}, V_n^{\mathrm{RS}})$, RS–RX pair $(V_n^{\mathrm{RS}}, V_i^{\mathrm{RX}})$, and CUE C_k^V are given by

$$\gamma^k_{V_i^{\mathrm{TX}},V_n^{\mathrm{RS}}}=\frac{P_{V_i^{\mathrm{TX}}}d^{-\alpha_v}_{V_i^{\mathrm{TX}},V_n^{\mathrm{RS}}}}{y_{k,f}P_{C_k^V}d^{-\alpha_{cv}}_{C_k^V,V_n^{\mathrm{RS}}}+N_0} \tag{2}$$

$$\gamma^k_{V_n^{\mathrm{RS}},V_i^{\mathrm{RX}}}=\frac{P_{V_n^{\mathrm{RS}}}d^{-\alpha_v}_{V_n^{\mathrm{RS}},V_i^{\mathrm{RX}}}}{(1-y_{k,f})P_{C_k^V}d^{-\alpha_{cv}}_{C_k^V,V_i^{\mathrm{RX}}}+N_0} \tag{3}$$

$$\gamma_k=\frac{P_{C_k^V}d^{-\alpha_c}_{C_k^V,B}}{y_{k,f}P_{V_i^{\mathrm{TX}}}d^{-\alpha_{vc}}_{V_i^{\mathrm{TX}},B}+(1-y_{k,f})P_{V_n^{\mathrm{RS}}}d^{-\alpha_{vc}}_{V_n^{\mathrm{RS}},B}+N_0} \tag{4}$$

where $P_{V_i^{\mathrm{TX}}}$, $P_{V_n^{\mathrm{RS}}}$, and $P_{C_k^V}$ denote the transmission power of V_i^{TX}, V_n^{RS}, and C_k^V, respectively. $d_{V_i^{\mathrm{TX}},V_n^{\mathrm{RS}}}$, $d_{V_n^{\mathrm{RS}},V_i^{\mathrm{RX}}}$, $d_{C_k^V,B}$, $d_{C_k^V,V_n^{\mathrm{RS}}}$, $d_{V_i^{\mathrm{TX}},B}$, and $d_{V_n^{\mathrm{RS}},B}$ are the transmission distances of TX–RS pair $(V_i^{\mathrm{TX}}, V_n^{\mathrm{RS}})$, RS–RX pair $(V_n^{\mathrm{RS}}, V_i^{\mathrm{RX}})$, cellular link from C_k^V to the base station, interference link $(C_k^V, V_n^{\mathrm{RS}})$, interference link from V_i^{TX} to the base station, and interference link from V_n^{RS} to the base station, respectively. α_v, α_c, α_{cv}, and α_{vc} represent the path-loss exponents of D2D–V2V link, cellular link, interference link from CUE to D2D–V2V pair, and interference link from D2D–V2V pair to base station, respectively. N_0 is the one-sided power spectral density of additive white Gaussian noise.

The effective SINR of the two-hop D2D–V2V pair $(V_i^{\mathrm{TX}}, V_n^{\mathrm{RS}}, V_i^{\mathrm{RX}})$ is denoted as $\gamma^k_{i,n}$, which is given by

$$\gamma^k_{i,n}=\frac{\gamma^k_{V_i^{\mathrm{TX}},V_n^{\mathrm{RS}}}\gamma^k_{V_n^{\mathrm{RS}},V_i^{\mathrm{RX}}}}{\gamma^k_{V_i^{\mathrm{TX}},V_n^{\mathrm{RS}}}+\gamma^k_{V_n^{\mathrm{RS}},V_i^{\mathrm{RX}}}+1}. \tag{5}$$

Remark 2: How to derive (5) is omitted here due to space limitations. A similar proof can be found in [20] and [32] and references therein.

Hence, after the two-hop D2D–V2V transmission, the energy efficiency $\mathrm{EE}_{i,n,k}$ (b/Hz/J) corresponding to $(V_i^{\mathrm{TX}}, V_n^{\mathrm{RS}}, V_i^{\mathrm{RX}})$ and C_k^V can be calculated as

$$\mathrm{EE}_{i,n,k}=\frac{\log_2(1+\gamma^k_{i,n})}{P_{V_i^{\mathrm{TX}}}+P_{V_n^{\mathrm{RS}}}+3P_{\mathrm{cir},v}}+\frac{\log_2(1+\gamma_k)}{P_{C_k^V}+P_{\mathrm{cir},c}} \tag{6}$$

where $P_{\mathrm{cir},v}$ and $P_{\mathrm{cir},c}$ are the transmission circuit power corresponding to vehicles and CUEs, respectively.

If either a proper V-RS or resource block cannot be found for $(V_i^{\mathrm{TX}}, V_i^{\mathrm{RX}})$, then the request of V_i^{RX} will be served by the base station using orthogonal downlink cellular spectrum. The corresponding SINR expression is given by

$$\gamma_{i,B}=\frac{P_{B,i}d^{-\alpha_c}_{B,V_i^{\mathrm{RX}}}}{N_0} \tag{7}$$

where $P_{B,i}$ and $d_{B,V_i^{\mathrm{RX}}}$ denote the transmission power and distance from the base station to V_i^{RX}, respectively.

Denote the set of V-RXs that are served by the base station as $\Omega_{\mathrm{RX},B}$, the energy efficiency of the base station is calculated as

$$\mathrm{EE}_B=\frac{\sum_{V_j^{\mathrm{RX}}\in\Omega_{\mathrm{RX},B}}\log_2(1+\gamma_{i,B})}{\sum_{V_j^{\mathrm{RX}}\in\Omega_{\mathrm{RX},B}}(P_{B,j}+P_{\mathrm{cir},v})+P_{\mathrm{cir},B}} \tag{8}$$

where $P_{\mathrm{cir},B}$ is the circuit power of the base station.

III. Problem Formulation

The objective of this paper is to achieve effective data offloading via cooperative two-hop D2D–V2V transmission with possible maximum network energy efficiency. It is higher priority that V-RXs are initially served by V-TXs via D2D–V2V transmission if possible. Only those V-RXs that cannot support two-hop D2D–V2V transmission are served by the base station. Hence, the energy-efficient resource allocation problem can be divided into two stages. In the first stage, the vehicular relay selection, spectrum resource allocation, and transmission power control are jointly optimized to maximize the energy efficiency of two-hop D2D–V2V pairs and CUEs. In the second stage, the transmission power of the base station is optimized in an energy-efficient way to serve those V-RXs via cellular links.

The set of optimization variables is defined as $\{\mathcal{Y},\mathcal{S},\mathcal{P}_{\mathrm{TX}},\mathcal{P}_{\mathrm{RS}},\mathcal{P}_B\}$. $\mathcal{Y}$ is the set of hop selection variables, i.e., $\mathcal{Y}=\{y_{1,f},y_{2,f},\ldots,y_{k,f},\ldots,y_{K,f}\}$. $\mathcal{S}$ is a $M\times N\times K$ matrix $\mathbf{S}_{M\times N\times K}$. Each binary element $s_{i,n,k}$ of the matrix $\mathbf{S}_{M\times N\times K}$ denotes the matching relationship among TX–RX pair $(V_i^{\mathrm{TX}}, V_i^{\mathrm{RX}})$, V-RS V_n^{RS}, and resource block C_k^{RB}. More specifically, $s_{i,n,k}=1$ represents that $(V_i^{\mathrm{TX}}, V_i^{\mathrm{RX}})$ and V_n^{RS} form a two-hop D2D–V2V link by reusing C_k^{RB}, and $s_{i,n,k}=0$, otherwise. $\mathcal{P}_{\mathrm{TX}}$, $\mathcal{P}_{\mathrm{RS}}$, and $\mathcal{P}_B$ are the set of transmission power corresponding to V-TXs, V-RSs, and the base station, i.e., $\mathcal{P}_{\mathrm{TX}}=\{P_{V_1^{\mathrm{TX}}},\ldots,P_{V_M^{\mathrm{TX}}}\}$, $\mathcal{P}_{\mathrm{RS}}=\{P_{V_1^{\mathrm{RS}}},\ldots,P_{V_N^{\mathrm{RS}}}\}$, and $\mathcal{P}_B=\{P_{B,i}\mid\forall V_i^{\mathrm{RX}}\in\Omega_{\mathrm{RX},B}\}$.

The first-stage energy-efficient joint optimization problem is formulated as

$$\mathbf{P_1}:\max_{\{\mathcal{S},\mathcal{P}_{\mathrm{TX}},\mathcal{P}_{\mathrm{RS}},\mathcal{Y}\}}\sum_{k=1}^{K}\sum_{n=1}^{N}\sum_{i=1}^{M}s_{i,n,k}\mathrm{EE}_{i,n,k}$$

$$\text{s.t. } C_1: s_{i,n,k},y_{k,f}\in\{0,1\}\quad\forall V_i^{\mathrm{TX}}\in\mathcal{V}_{\mathrm{TX}},$$
$$V_n^{\mathrm{RS}}\in\mathcal{V}_{\mathrm{RS}},V_i^{\mathrm{RX}}\in\mathcal{V}_{\mathrm{RX}},C_k^{\mathrm{RB}}\in\mathcal{C}_{\mathrm{RB}}$$

$$C_2:\sum_{V_n^{\mathrm{RS}}\in\mathcal{V}_{\mathrm{RS}},C_k^{\mathrm{RB}}\in\mathcal{C}}s_{i,n,k}\le 1\quad\forall V_i^{\mathrm{TX}}\in\mathcal{V}_{\mathrm{TX}}$$

$$C_3:\sum_{V_i^{\mathrm{TX}}\in\mathcal{V}_{\mathrm{TX}},C_k^{\mathrm{RB}}\in\mathcal{C}}s_{i,n,k}\le 1\quad\forall V_n^{\mathrm{RS}}\in\mathcal{V}_{\mathrm{RS}}$$

$$
\begin{aligned}
&C_4: \sum_{V_i^{\mathrm{TX}}\in\mathcal{V}_{\mathrm{TX}}, V_n^{\mathrm{RS}}\in\mathcal{V}_{\mathrm{RS}}} s_{i,n,k} \le 1 \quad \forall C_k^{\mathrm{RB}} \in \mathcal{C}_{\mathrm{RB}} \\
&C_5: \min(\gamma^k_{V_i^{\mathrm{TX}},V_n^{\mathrm{RS}}}, \gamma^k_{V_n^{\mathrm{RS}},V_i^{\mathrm{RX}}}, \gamma^k_{i,n}) \ge \gamma^V_{\min}, \\
&\quad \gamma_k \ge \gamma^C_{\min} \quad \forall C_k^V \in \mathcal{C}_V \\
&C_6: 0 \le P_{V_i^{\mathrm{TX}}} \le P^V_{\max} \quad \forall V_i^{\mathrm{TX}} \in \mathcal{V}_{\mathrm{TX}}, \\
&\quad 0 \le P_{V_n^{\mathrm{RS}}} \le P^V_{\max} \quad \forall V_n^{\mathrm{RS}} \in \mathcal{V}_{\mathrm{RS}}. \qquad (9)
\end{aligned}
$$

Hence, we have $|\,\Omega_{\mathrm{RX},B}\,| = \sum_{i=1}^{M}(1-\sum_{k=1}^{K}\sum_{n=1}^{N} s_{i,n,k})$, where $|\,\Omega_{\mathrm{RX},B}\,|$ is the number of elements in $\Omega_{\mathrm{RX},B}$. The second-stage energy-efficient power control problem is given by

$$
\begin{aligned}
&\mathbf{P_2}: \max_{\{\mathcal{P}_{\mathbf{B}}\}} \mathrm{EE}_B, \\
&\text{s.t. } C_7: \gamma_{i,B} \ge \gamma^V_{\min} \quad \forall V_i^{\mathrm{RX}} \in \Omega_{\mathrm{RX},B} \\
&\quad C_8: \sum_{i=1}^{M}\left(1-\sum_{k=1}^{K}\sum_{n=1}^{N} s_{i,n,k}\right) P_{B,i} \le P^B_{\max}, \\
&\quad P_{B,i} \ge 0 \quad \forall V_i^{\mathrm{RX}} \in \Omega_{\mathrm{RX},B}. \qquad (10)
\end{aligned}
$$

Here, C_1–C_4 ensure that there is a one-to-one matching among any TX–RX pair $(V_i^{\mathrm{TX}}, V_i^{\mathrm{RX}})$, V-RS V_n^{RS}, and resource block C_k^{RB}, $\forall V_i^{\mathrm{TX}} \in \mathcal{V}_{\mathrm{TX}}, V_n^{\mathrm{RS}} \in \mathcal{V}_{\mathrm{RS}}, V_i^{\mathrm{RX}} \in \mathcal{V}_{\mathrm{RX}}, C_k^{\mathrm{RB}} \in \mathcal{C}$. C_5 and C_7 ensure that the QoS requirements of both D2D–V2V links and cellular links should be satisfied simultaneously. $\gamma^V_{\min}$ and $\gamma^C_{\min}$ denote the SINR threshold for any D2D–V2V link and cellular link, respectively. C_6 and C_8 specify the transmission power constraints for V-TXs, V-RSs, and the base station. $P^V_{\max}$ and $P^B_{\max}$ denote the transmission power threshold for any D2D–V2V transmitter and the base station, respectively.

IV. Two-Stage Energy-Efficient Resource Allocation

In this section, we first introduce an auction-matching-based energy-efficient resource allocation algorithm to address the first-stage joint optimization problem. Then, a nonlinear fractional programming based power allocation algorithm is derived in the second stage. Finally, we provide an in-depth analysis of theoretical properties.

A. Auction-Matching-Based Energy-Efficient Resource Allocation

Since problem $\mathbf{P_1}$ involves a matching among three sides, i.e., TX–RX pairs, V-RSs, and resource blocks, a V-RS and a resource block can be combined as a RS-resource block (RS–RB) group to reduce the complexity of the three-sided matching problem. With N V-RSs and K resource blocks, a total of $N \times K$ possible combinations can be created, the set of which is denoted as $\mathcal{V}_{\mathrm{RS,RB}} = \{V_{n,k}^{\mathrm{RS,RB}}\}_{n=1,k=1}^{n=N,k=K}$. Thus, (9) is reduced to a two-sided matching problem with M TX–RX pairs on one side and $N \times K$ RS–RB groups on the other side. We define φ as a one-to-one matching, which is a one-to-one mapping from the set $\{\mathcal{V}_{\mathrm{TX}}, \mathcal{V}_{\mathrm{RX}}\} \cup \mathcal{V}_{\mathrm{RS,\,RB}}$ to the set $\{\mathcal{V}_{\mathrm{TX}}, \mathcal{V}_{\mathrm{RX}}\} \cup \mathcal{V}_{\mathrm{RS,\,RB}} \cup \{\emptyset\}$. $\varphi(i) = V_{n,k}^{\mathrm{RS,\,RB}}$ represents that TX–RX pair $(V_i^{\mathrm{TX}}, V_i^{\mathrm{RX}})$ is matched with RS–RB group $V_{n,k}^{\mathrm{RS,\,RB}}$.

In the two-sided matching process, M TX–RX pairs and $N \times K$ RS–RB groups are matched with each other based on preferences. We denote $\Phi_{\mathrm{RS}} = \{\phi_1^{\mathrm{RS}}, \ldots, \phi_n^{\mathrm{RS}}, \ldots, \phi_N^{\mathrm{RS}}\}$ and $\Phi_{\mathrm{RB}} = \{\phi_1^{\mathrm{RB}}, \ldots, \phi_k^{\mathrm{RB}}, \ldots, \phi_K^{\mathrm{RB}}\}$ as the price sets of V-RSs and resource blocks, respectively. For example, ϕ_n^{RS} represents the matching cost for any TX–RX pair that prefers to be paired with V-RS V_n^{RS}. The initial value of any $\phi_n^{\mathrm{RS}} \in \Phi_{\mathrm{RS}}$ and any $\phi_k^{\mathrm{RB}} \in \Phi_{\mathrm{RB}}$ can be set as the same just for simplicity purpose. The preference value of $(V_i^{\mathrm{TX}}, V_i^{\mathrm{RX}})$ toward any $V_{n,k}^{\mathrm{RS,\,RB}} \in \mathcal{V}_{\mathrm{RS,\,RB}}$ is defined as the achievable network energy efficiency minus the total matching cost, which is given by

$$
U_{i,n,k} = \mathrm{EE}_{i,n,k} - \phi_n^{\mathrm{RS}} - \phi_k^{\mathrm{RB}} \qquad (11)
$$

where $\mathrm{EE}_{i,n,k}$ is calculated by solving the following power control problem

$$
\begin{aligned}
&\mathbf{P_3}: \max_{\{P_{V_i^{\mathrm{TX}}}, P_{V_n^{\mathrm{RS}}}\}} \mathrm{EE}_{i,n,k} \\
&\text{s.t.} \qquad \tilde{C}_5, \tilde{C}_6 \qquad (12)
\end{aligned}
$$

where $\tilde{C}_5$ and $\tilde{C}_6$ are special version of C_5 and C_6, respectively, in which only the constraints related to V_i^{TX}, V_n^{RS}, V_i^{RX}, and C_k^V are considered. $\mathbf{P_3}$ is jointly concave with $P_{V_i^{\mathrm{TX}}}$ and $P_{V_n^{\mathrm{RS}}}$, and can be solved by Lagrange dual decomposition. The detailed solution derivation process is omitted here due to space limitation. After obtaining $U_{i,n,k}$ for any RS–RB group, the preference list of $(V_i^{\mathrm{TX}}, V_i^{\mathrm{RX}})$ is generated by sorting all of RS–RB groups in a descending order according to preference values, which is denoted as the set Ψ_i.

The two-sided matching is implemented in an iterative fashion. In each matching iteration, any TX–RX pair $(V_i^{\mathrm{TX}}, V_i^{\mathrm{RX}})$ that has not been matched sends a proposal to the top-ranking RS–RB in the set Ψ_i, e.g., $V_{n,k}^{\mathrm{RS,\,RB}}$. If $V_{n,k}^{\mathrm{RS,\,RB}}$ only receives a proposal from $(V_i^{\mathrm{TX}}, V_i^{\mathrm{RX}})$, then a stable matching is obtained by simply pairing $(V_i^{\mathrm{TX}}, V_i^{\mathrm{RX}})$ with its most preferred RS–RB group $V_{n,k}^{\mathrm{RS,\,RB}}$. Otherwise, if more than one TX–RX pair request to be matched with the same V-RS or resource block, an English auction approach is adopted for matching conflict avoidance and preference updating.

In English auction, the current bid is increased by a predefined increment in each round of new bidding, and the highest bidder needs to win by outbidding the next-highest bidder with the minimum increment. The auction model consists of the following four elements.

1) Auction goods: Let $\mathcal{G}$ denote the set of V-RSs and resource blocks that receive multiple proposals. The elements of $\mathcal{G}$ are the goods to be auctioned.
2) Auctioneer: The base station acts as an auctioneer and determines how to allocate the elements of $\mathcal{G}$ to bidders based on the auction rules.
3) Bidders: Let $\mathcal{B}$ denote the set of TX–RX pairs involved in matching conflicts, which is also the set of bidders.
4) Bidding price: The sets of bidding prices for V-RSs and resource blocks are Φ_{RS} and Φ_{RB}, respectively. In each new round of bidding, the sets of price increment for Φ_{RS}

and Φ_{RB} are denoted as

$$\Delta\Phi_{\mathrm{RS}} = \{\Delta\phi_1^{\mathrm{RS}}, \ldots, \Delta\phi_n^{\mathrm{RS}}, \ldots, \Delta\phi_N^{\mathrm{RS}}\},$$

and

$$\Delta\Phi_{\mathrm{RB}} = \{\Delta\phi_1^{\mathrm{RB}}, \ldots, \Delta\phi_k^{\mathrm{RB}}, \ldots, \Delta\phi_K^{\mathrm{RB}}\},$$

respectively.

For any element of $\mathcal{G}$, an auction is held to determine which TX–RX pair is the winner. Assuming both $(V_i^{\mathrm{TX}}, V_i^{\mathrm{RX}})$ and $(V_j^{\mathrm{TX}}, V_j^{\mathrm{RX}})$ compete for the same V-RS V_n^{RS}, $(V_i^{\mathrm{TX}}, V_i^{\mathrm{RX}}), (V_j^{\mathrm{TX}}, V_j^{\mathrm{RX}}) \in \mathcal{B}$, $V_n^{\mathrm{RS}} \in \mathcal{G}$. Define l_b as the index of bidding iteration. In the (l_b+1)th bidding round, the bidding price of bidders toward V_n^{RS} is increased by $\Delta\phi_n^{\mathrm{RS}}$, i.e.,

$$\phi_n^{\mathrm{RS}}(l_b+1) = \phi_n^{\mathrm{RS}}(l_b) + \Delta\phi_n^{\mathrm{RS}}. \tag{13}$$

Combining (11) and (13), the preferences of $(V_i^{\mathrm{TX}}, V_i^{\mathrm{RX}})$ and $(V_j^{\mathrm{TX}}, V_j^{\mathrm{RX}})$ toward V_n^{RS} are also reduced by $\Delta\phi_n^{\mathrm{RS}}$, and the preference lists Ψ_i and Ψ_j are updated by reordering candidate RS–RB groups. As ϕ_n^{RS} is increased by $\Delta\phi_n^{\mathrm{RS}}$ in each bidding round, a bidder will give up V_n^{RS} if V_n^{RS} no longer belongs to its most preferred RS–RB group. The bidder will quit the auction and send a new proposal to its currently most preferred RS–RB group. The bidding process terminates when no bidder is willing to outbid the current bidding price, and the base station allocates V_n^{RS} to the TX–RX pair that placed the current bid.

Finally, the matching process will continue until none TX–RX pair can been matched with any RS–RB group. Then, the V-RXs that cannot support D2D–V2V transmission will be served by the base station via downlink cellular links.

B. Nonlinear Fractional Programming Based Energy-Efficient Power Control

Since EE_B is defined in fractional form, we employ nonlinear fractional programming to transform problem $\mathbf{P_2}$ into an equivalent convex problem with a subtractive-form objective function. Denote $R_{\mathrm{total},B}(\mathcal{P}_B)$ and $P_{\mathrm{total},B}(\mathcal{P}_B)$ as $\sum_{V_j^{\mathrm{RX}}\in\Omega_{\mathrm{RX},B}} \log_2(1+\gamma_{i,B})$ and $\sum_{V_j^{\mathrm{RX}}\in\Omega_{\mathrm{RX},B}} (P_{B,j} + P_{\mathrm{cir},v}) + P_{\mathrm{cir},B}$, respectively. Define EE_B^* as the optimum objective value, which is given by

$$\mathrm{EE}_i^{B*} = \max_{\mathcal{P}_B} \mathrm{EE}_B = \frac{R_{\mathrm{total},B}(\mathcal{P}_B^*)}{P_{\mathrm{total},B}(\mathcal{P}_B^*)} \tag{14}$$

where $\mathcal{P}_B^*$ denotes the optimum transmission power strategy. Based on [12], we have the following property.

Theorem 1: EE_B^* is achieved if and only if

$$\max_{\mathcal{P}_B} R_{\mathrm{total},B}(\mathcal{P}_B) - \mathrm{EE}_B^* P_{\mathrm{total},B}(\mathcal{P}_B)$$
$$= R_{\mathrm{total},B}(\mathcal{P}_B^*) - \mathrm{EE}_B^* P_{\mathrm{total},B}(\mathcal{P}_B^*) = 0. \tag{15}$$

Hence, $\max_{\mathcal{P}_B} R_{\mathrm{total},B}(\mathcal{P}_B) - \mathrm{EE}_B^* P_{\mathrm{total},B}(\mathcal{P}_B)$ is the equivalent problem of $\mathbf{P_2}$ in subtractive form. Both EE_B^* and $\mathcal{P}_B^*$ can be obtained iteratively as in Algorithm 1. In each iteration, the following problem is solved:

$$\mathbf{P_4}: \max_{\mathcal{P}_B} R_{\mathrm{total},B}(\mathcal{P}_B) - \mathrm{EE}_B P_{\mathrm{total},B}(\mathcal{P}_B)$$
$$\text{s.t.} \quad C_7, C_8. \tag{16}$$

Algorithm 1: The Iterative Power Control Algorithm.

```
Set maximum to tolerance δ;
while (!Convergence) do
    Solve problem P4 for a given EE_B and obtain P̃_B;
    if R_{total,B}(P̃_B) − EE_B P_{total,B}(P̃_B) ≤ δ then
        Convergence = true;
        return P*_B = P̃_B and obtain EE*_B by (14);
    else
        Convergence = false;
        return EE_B = R_{total,B}(P̃_B)/P_{total,B}(P̃_B);
    end if
end while
```

Readers can refer to [12] and references therein for more details.

C. Property Analysis

By employing the concept from the matching theory and nonlinear fractional programming [12], [16], [20], the following convergence and stability properties can be derived. The proof is omitted here due to space limitation.

Theorem 2: φ generated by the auction-matching-based resource allocation algorithm converges to a stable matching. EE_B generated by the nonlinear fractional programming based power control algorithm also converges to EE_B^* within finite iterations.

In the preference establishment process, the computational complexity for each TX–RX pair to acquire preferences is $\mathcal{O}(NK)$. The preference list can be derived by sorting the preference values for each TX–RX pair and the computational complexity is $\mathcal{O}(NK\log(NK))$ when taking N V-RSs and K RBs into consideration. Furthermore, the computational complexity of the matching process is $\mathcal{O}(MM^{N_b})$ when $M \geq \max(K,N)$, or $\mathcal{O}(KM^{N_b})$ when $\min(K,N) \geq M$, where N_b is the number of bidding rounds and M^{N_b} is the required number of iterations by the price rising process to resolve the conflict. Therefore, the total computational complexity of the auction-matching-based resource allocation algorithm is $\mathcal{O}(MNK\lceil\log(NK)+1\rceil + MM^{N_b})$ if $M \geq \max(K,N)$, or $\mathcal{O}(MNK\lceil\log(NK)+1\rceil + KM^{N_b})$ if $\min(K,N) \geq M$.

Furthermore, the total number of possible matching results in the ideal brute-force searching scheme is $((NK)^M M!)$, and the complexity can be derived as $\mathcal{O}((NK)^M M!)$. The complexity of the proposed scheme is much lower compared with the ideal brute-force searching scheme for sufficient large values of M, N, K. For example, when $M = 10, N = K = 12$, the complexity of the ideal brute-force searching scheme is 1.13×10^{18} times higher than that of the proposed scheme.

V. Performance Evaluation

In this section, we evaluate the proposed auction-matching-based energy-efficient resource allocation algorithm based on real-world road topology and realistic vehicular traffic. Both macromobility and micromobility features are taken into consideration. In the following, we first introduce experiment setup, and then provide numerical results.

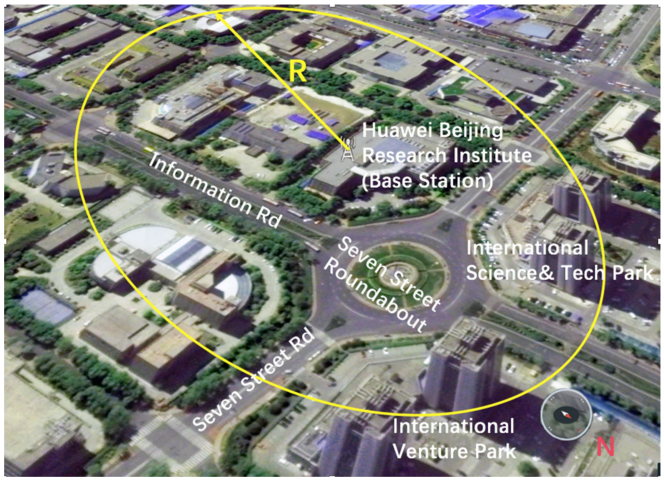

Fig. 2. Real-world road topology of the Seven Street area in the Shangdi area, Beijing, China.

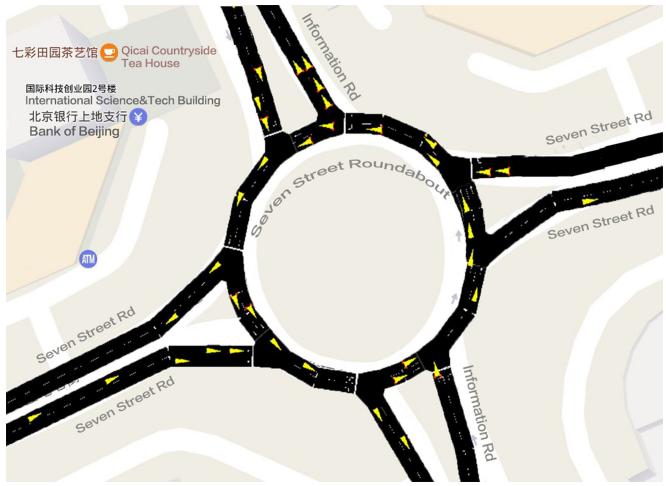

Fig. 3. Snapshot of SUMO simulation scenario based on the real-world road topology of the Seven Street roundabout, where vehicles are represented by small triangles.

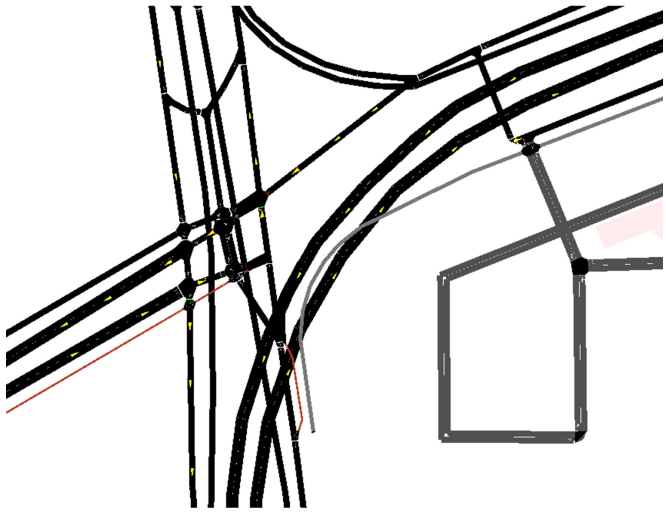

Fig. 4. Snapshot of the SUMO simulation scenario based on the Suzhou Viaduct.

A. Experiment Setup

We adopt the microscopic road traffic simulation software SUMO to evaluate vehicle traffics in real-world road topologies without having to deploy an expensive physical transportation measurement system. Fig. 2 shows the real-world road topology of the Seven Street in the Shangdi area, Beijing, China, which is located at 40 °N and 116 °E. The Seven Street is adopted as the evaluation scenario, where famous companies such as Baidu, Lenovo, and Huawei, are located. We use the road network importing tool of SUMO, i.e., NETCONVERT, to read data from OpenStreetMap and obtain the description of road graph in terms of nodes, edges, connection links, etc., as XML files.

In microscopic simulation environment, each vehicle is treated as a single element and controlled separately by setting its primate route, speed, acceleration, heading, and lane changing parameters. The RANDOMTRIPS tool is used to generate vehicles based on road situations, such as traffic congestion, signal of traffic light and intervehicle distance, and so on. The time step of the time-discrete space-continuous simulation is set as 0.1 s, and the total simulation duration is set as 10^3 s. Hence, a total of 10^4 different snapshots are generated. Fig. 3 shows a snapshot of SUMO simulation scenario based on the real-world road topology of the Seven Street roundabout, where vehicles are represented by small triangles. Furthermore, the real-world road topology of the Suzhou viaduct is adopted for comparison with the Seven Street area. Fig. 4 shows a snapshot of the SUMO simulation scenario based on the Suzhou Viaduct.

We further connect SUMO with external communication network simulation software MATLAB by exploring the traffic control interface protocols. We can run both SUMO and MATLAB simulations simultaneously and acquire various simulation parameters and attributes such as vehicle coordinate, departure time, speed, etc., via predefined standard interface. The proposed algorithm is compared with several heuristic algorithms, including the brute-force searching approach, the random resource allocation approach without power control, and the nonrelay-based spectrum-efficient resource allocation approach. A summary of simulation parameters is provided in Table I.

B. Numerical Results

Fig. 5 shows the average network energy efficiency of the overall heterogeneous network versus the number of D2D–V2V TX–RX pairs. TX–RX pair number is positively related to the performance gain, because increasing the number of TX–RX pairs brings proximity gain and spectrum reusing gain. When $M = 6$ and $N = 6$, the proposed algorithm can achieve up to 93% of the optimum performance, and outperform the nonrelay-based spectrum-efficient approach and the random allocation approach without power control by more than 36% and 67%, respectively. The reason lies behind is that relay selection, spectrum allocation, and power control are not jointly optimized from an energy efficiency perspective in the two heuristic algorithms.

TABLE I
SIMULATION PARAMETERS

Simulation Parameter	Value
Cell radius	500 m
Transmit power of CUEs $P_{C_k^V}$	20 dBm
Max transmit power of V-TXs and V-RSs $P^V_{\max}$	23 dBm
Max transmit power of base station $P^B_{\max}$	46 dBm
Path-loss exponent α_c, α_v, α_{cv}, α_{vc}	3, 3.5, 4, 3
Circuit power of vehicles and CUEs $P_{\text{cir},c}$, $P_{\text{cir},v}$	100, 200 mW
Circuit power of base station $P_{\text{cir},B}$	160 W
Noise power N_0	-114 dBm
Number of D2D–V2V pairs M	$1 \sim 10$
Number of D2D–V2V relay stations N	$1 \sim 10$
Number of resource blocks K	$1 \sim 10$
SINR threshold $\gamma^V_{\min}$, $\gamma^C_{\min}$	20 dB

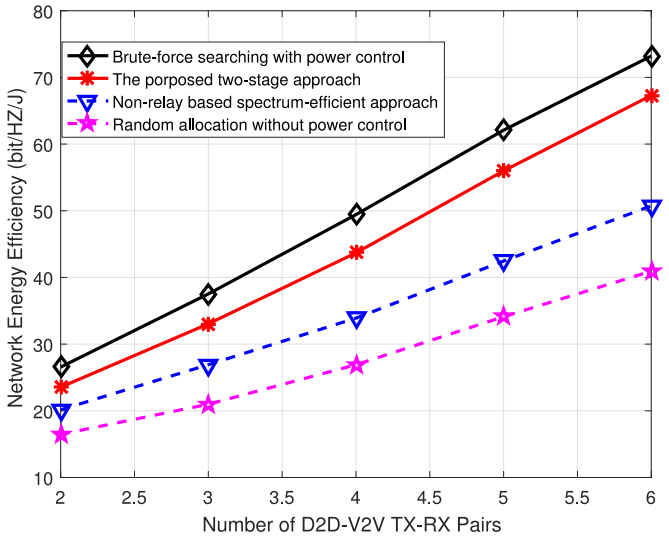

Fig. 5. Average network energy efficiency versus the number of D2D–V2V TX–RX pairs ($N = K = 6, M = 2 \sim 6$, $\gamma^V_{\min} = \gamma^C_{\min} = 20$ dB).

Figs. 6 and 7 show the percentage of V-RXs served by D2D–V2V transmission and the network energy efficiency performance versus different SINR thresholds, respectively. A V-RX can only be served via D2D–V2V transmission if and only if the achieved SINR is above the specified SINR threshold. The proposed algorithm achieves superior performances in both network coverage and energy efficiency due to the joint optimization of vehicular and wireless resources. It is noted that both the percentage of served V-RXs and the energy efficiency performance decrease along with SINR threshold, because it is more difficult to find appropriate RS–RB groups that can satisfy increasing QoS requirements.

Fig. 8 shows the percentage of energy saving versus the involvement factor of D2D–V2V-enabled vehicles. Clearly, as more vehicles operate in D2D–V2V mode, great energy saving gains can be achieved compared to the baseline operation (all vehicles operate in cellular mode). Hence, it is exceptionally beneficial to employ D2D–V2V transmission for green cities. However, the scaling of the energy saving gain with the involvement factor is bounded primarily by two constraints, i.e., SINR threshold and spectrum resource. Therefore, the result is

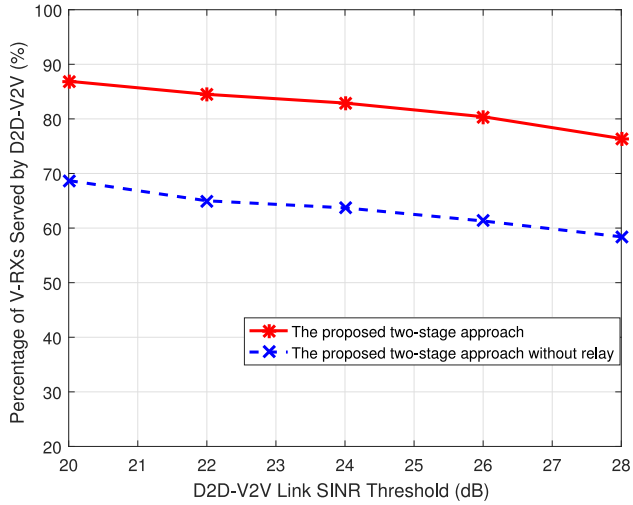

Fig. 6. Average percentage of V-RXs served by D2D–V2V transmission versus different SINR thresholds of D2D–V2V link ($N = 10, K = 10, M = 10$, $\gamma^V_{\min} = 20 \sim 28$ dB).

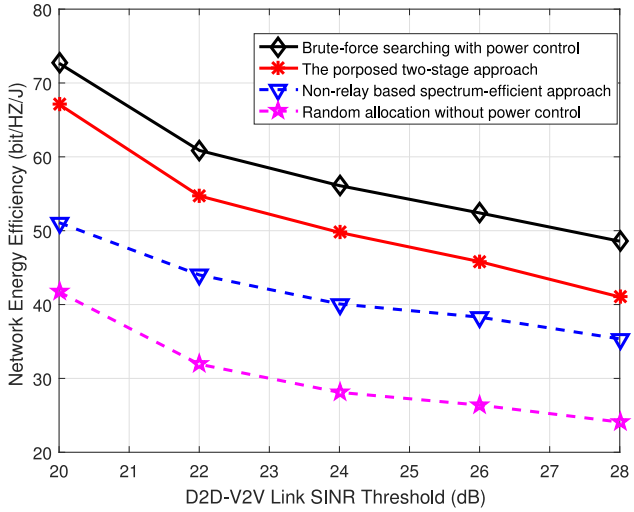

Fig. 7. Average network energy efficiency versus different SINR thresholds of D2D–V2V link ($N = 6, K = 6, M = 6$, $\gamma^V_{\min} = 20 \sim 28$ dB).

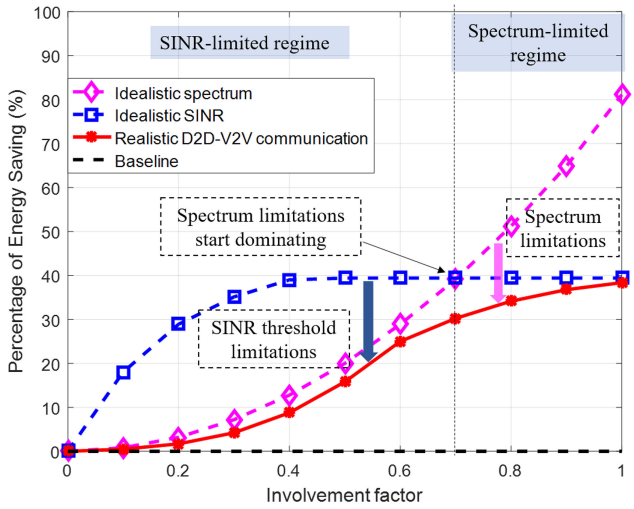

Fig. 8. Percentage of energy saving versus involvement factor (100 vehicles, $K = 20$, $\gamma^V_{\min} = \gamma^C_{\min} = 20$ dB).

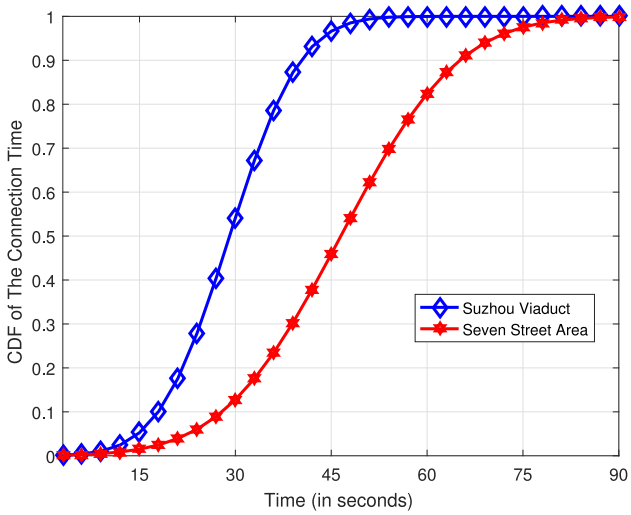

Fig. 9. CDF of the connection time versus connection time threshold.

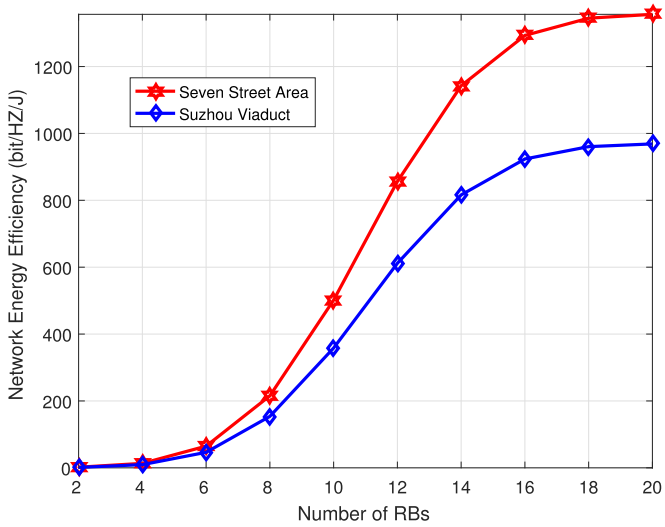

Fig. 10. Average network energy efficiency versus the number of resource blocks (100 vehicles, $\gamma_{\min}^{V} = \gamma_{\min}^{C} = 20$ dB).

compared with two extreme cases, i.e., the idealistic D2D–V2V link scenario without any SINR threshold constraint and the idealistic spectrum scenario with adequate resource blocks. In the SINR-limited regime, there are too few D2D–V2V-enabled vehicles available in the network, and it is difficult to find suitable reliable vehicular connections that satisfy the SINR threshold. As the involvement factor increases, the performance enters the spectrum-limited regime, where the network does not have any resource block to accept additional D2D–V2V link establishment. Thus, proper consideration of SINR and spectrum-related performance limitations are required to achieve satisfactory energy saving gains.

Fig. 9 shows the CDF of the connection time versus the connection time threshold. The average headway distance between two vehicles in the Suzhou Viaduct is larger than that in the Seven Street area due to the fact that the mean value of velocity in the Suzhou Viaduct scenario is higher. Hence, as the initial headway distance increases, it is more likely for two vehicles to move out of the communication range, which results in lower connection probability. For example, when the connection time threshold is 45 s, the probabilities that the connection duration of two vehicles is less than the connection time threshold are 47% and 98% for the Seven Street and Suzhou Viaduct scenarios, respectively.

Fig. 10 shows the average network energy efficiency versus the number of RBs. Numerical results demonstrate that the average network energy efficiency increases along with the number of RBs. In the beginning, significant performance gains can be achieved since additional D2D–V2V pairs can be supported by add more RBs. However, the performance improvement becomes saturated when the number of RBs is sufficiently large, i.e., no more D2D–V2V pairs are available. Furthermore, the performance achieved in the Seven Street scenario is generally better than that of the Suzhou Viaduct scenario due to the fact that the former has larger connection probability, which will increase the number of D2D–V2V pairs that are eligible for the cooperative two-hop D2D–V2V transmission.

VI. Conclusion

In this paper, a two-stage resource allocation algorithm was proposed for realizing energy-efficient vehicular heterogeneous networks in green cities. In the first stage, we proposed an auction-matching-based joint relay selection, spectrum allocation, and power control algorithm to optimize the energy efficiency of two-hop D2D–V2V and cellular links simultaneously in an iterative fashion. In the second stage, a nonlinear fractional programming based power control algorithm was developed to maximize the energy efficiency of the base station. The superiority of the proposed algorithm was validated based on real-world road topology and realistic vehicular traffic. In the future, we will consider the joint content caching and dissemination optimization problem in D2D-based cooperative vehicular networks.

References

[1] Y. Zhang, R. Yu, M. Nekovee, Y. Liu, S. Xie, and S. Gjessing, "Cognitive machine-to-machine communications: Visions and potentials for the smart grid," *IEEE Netw.*, vol. 26, no. 3, pp. 6–13, May 2012.

[2] Z. Zhou, J. Gong, Y. He, and Y. Zhang, "Software defined machine-to-machine communication for smart energy management," *IEEE Commun. Mag.*, vol. 55, no. 10, pp. 52–60, Apr. 2017.

[3] P. M. d'Orey and M. Ferreira, "ITS for sustainable mobility: A survey on applications and impact assessment tools," *IEEE Trans. Intell. Transp. Syst.*, vol. 15, no. 2, pp. 477–493, Apr. 2014.

[4] S. Maharjan, Q. Zhu, Y. Zhang, S. Gjessing, and T. Basar, "Dependable demand response management in the smart grid: A Stackelberg game approach," *IEEE Trans. Smart Grid*, vol. 4, no. 1, pp. 120–132, Mar. 2013.

[5] J. Cheng, W. Wu, J. Cao, and K. Li, "Fuzzy group-based intersection control via vehicular networks for smart transportations," *IEEE Trans. Ind. Informat.*, vol. 13, no. 2, pp. 751–758, Apr. 2017.

[6] H. Liu, H. Ning, Y. Zhang, and T. Yang, "Aggregated-proofs based privacy-preserving authentication for V2G networks in the smart grid," *IEEE Trans. Smart Grid*, vol. 3, no. 4, pp. 1722–1733, Dec. 2012.

[7] K. Lin, J. Luo, L. Hu, M. S. Hossain, and A. Ghoneim, "Localization based on social big data analysis in the vehicular networks," *IEEE Trans. Ind. Informat.*, vol. 13, no. 4, pp. 1932–1940, Aug. 2017.

[8] Z. Zhou, C. Sun, R. Shi, Z. Chang, S. Zhou, and Y. Li, "Robust energy scheduling in vehicle-to-grid networks," *IEEE Netw.*, vol. 31, no. 2, pp. 30–37, Mar. 2017.

[9] X. Cao, L. Liu, Y. Cheng, L. X. Cai, and C. Sun, "On optimal device-to-device resource allocation for minimizing end-to-end delay in VANETs," *IEEE Trans. Veh. Technol.*, vol. 65, no. 10, pp. 7905–7916, Oct. 2016.

[10] X. Cheng, L. Yang, and X. Shen, "D2D for intelligent transportation systems: A feasibility study," *IEEE Trans. Intell. Transp. Syst.*, vol. 16, no. 4, pp. 1784–1793, Aug. 2015.

[11] Y. Ren, F. Liu, Z. Liu, C. Wang, and Y. Ji, "Power control in D2D-based vehicular communication networks," *IEEE Trans. Veh. Technol.*, vol. 64, no. 12, pp. 5547–5562, Dec. 2015.

[12] Z. Zhou, M. Dong, K. Ota, and C. Xu, "Energy-efficient matching for resource allocation in D2D enabled cellular networks," *IEEE Trans. Veh. Technol.*, vol. 66, no. 6, pp. 5256–5268, Jun. 2017.

[13] R. Zhang, X. Cheng, L. Yang, and B. Jiao, "Interference graph-based resource allocation (InGRA) for D2D communications underlaying cellular networks," *IEEE Trans. Veh. Technol.*, vol. 64, no. 8, pp. 3844–3850, Aug. 2015.

[14] N. Cheng *et al.*, "Performance analysis of vehicular device-to-device underlay communication," *IEEE Trans. Veh. Technol.*, vol. 66, no. 6, pp. 5409–5421, Jun. 2017.

[15] R. Zhang, X. Cheng, L. Yang, X. Shen, and B. Jiao, "A novel centralized TDMA-based scheduling protocol for vehicular networks," *IEEE Trans. Intell. Transp. Syst.*, vol. 16, no. 1, pp. 411–416, Feb. 2015.

[16] Z. Zhou, C. Gao, C. Xu, Y. Zhang, S. Mumtaz, and J. Rodriguez, "Social big data based content dissemination in internet of vehicles," *IEEE Trans. Ind. Informat.*, vol. PP, no. 99, pp. 1–1, Jul. 2017.

[17] C. Wu, S. Ohzahata, Y. Ji, and T. Kato, "Joint fuzzy relays and network-coding-based forwarding for multihop broadcasting in VANETs," *IEEE Trans. Intell. Transp. Syst.*, vol. 16, no. 3, pp. 1415–1427, Jun. 2015.

[18] M. Hu, J. Luo, Y. Wang, M. Lukasiewycz, and Z. Zeng, "Holistic scheduling of real-time applications in time-triggered in-vehicle networks," *IEEE Trans. Ind. Informat.*, vol. 10, no. 3, pp. 1817–1828, Aug. 2014.

[19] Y. Zhang, R. Yu, S. Xie, W. Yao, Y. Xiao, and M. Guizani, "Home M2M networks: Architectures, standards, and QoS improvement," *IEEE Commun. Mag.*, vol. 49, no. 4, pp. 0163–6804, Apr. 2011.

[20] C. Xu, J. Feng, B. Huang, Z. Zhou, S. Mumtaz, and J. Rodriguez, "Joint relay selection and resource allocation for energy-efficient D2D cooperative communications using matching theory," *Appl. Sci.*, vol. 7, no. 5, pp. 1–24, 2017.

[21] J. Hrri, M. Fiore, F. Fethi, and C. Bonnet, "Vanetmobisim: Generating realistic mobility patterns for VANETs," in *Proc. ACM SIGMOBILE*, Los Angeles, CA, USA, Sep. 2006, pp. 1–2.

[22] S. Xiao, X. Zhou, D. Feng, Y. Wu, G. Li, and W. Guo, "Energy-efficient mobile association in heterogeneous networks with device-to-device communications," *IEEE Trans. Wireless Commun.*, vol. 15, no. 8, pp. 5260–5271, Aug. 2016.

[23] Y. Yang, Y. Zhang, L. Dai, J. Li, S. Mumtaz, and J. Rodriguez, "Transmission capacity analysis of relay-assisted device-to-device overlay/underlay communication," *IEEE Trans. Ind. Informat.*, vol. 13, no. 1, pp. 380–389, Feb. 2017.

[24] M. Feteiha and H. Hassanein, "Enabling cooperative relaying VANET clouds over LTE-A networks," *IEEE Trans. Veh. Technol.*, vol. 64, no. 4, pp. 1468–1479, Apr. 2015.

[25] S. Bharati and W. Zhuang, "CRB: Cooperative relay broadcasting for safety applications in vehicular networks," *IEEE Trans. Veh. Technol.*, vol. 65, no. 12, pp. 9542–9553, Dec. 2016.

[26] Y. Ge, S. Wen, Y. Ang, and Y. Liang, "Optimal relay selection in IEEE 802.16j multihop relay vehicular networks," *IEEE Trans. Veh. Technol.*, vol. 59, no. 5, pp. 2198–2206, Jun. 2010.

[27] W. He, G. Yan, and L. D. Xu, "Developing vehicular data cloud services in the IoT environment," *IEEE Trans. Ind. Informat.*, vol. 10, no. 2, pp. 1587–1595, May 2014.

[28] Y. Gu, W. Saad, M. Bennis, M. Debbah, and Z. Han, "Matching theory for future wireless networks: Fundamentals and applications," *IEEE Commun. Mag.*, vol. 53, no. 5, pp. 52–59, May 2015.

[29] X. Feng *et al.*, "Cooperative spectrum sharing in cognitive radio networks: A distributed matching approach," *IEEE Trans. Commun.*, vol. 62, no. 8, pp. 2651–2664, Aug. 2014.

[30] G. Yan and S. Olariu, "A probabilistic analysis of link duration in vehicular ad hoc networks," *IEEE Trans. Intell. Transp. Syst.*, vol. 12, no. 4, pp. 1227–1236, Dec. 2011.

[31] T. H. Luan, X. Shen, F. Bai, and L. Sun, "Feel bored? join verse! engineering vehicular proximity social networks," *IEEE Trans. Veh. Technol.*, vol. 64, no. 3, pp. 1120–1131, Mar. 2015.

[32] H. Xiao, Y. Hu, K. Yan, and S. Ouyang, "Power allocation and relay selection for multisource multirelay cooperative vehicular networks," *IEEE Trans. Intell. Transp. Syst.*, vol. 17, no. 11, pp. 3297–3305, Nov. 2016.

Zhenyu Zhou (M'11–SM'17) received the M.E. and Ph.D. degrees in communication engineering from Waseda University, Tokyo, Japan, in 2008 and 2011, respectively.

Since March 2013, he has been an Associate Professor at North China Electric Power University, Beijing, China. His research interests include green communications and smart grid.

Dr. Zhou is an Editor of the IEEE ACCESS and the *IEEE Communications Magazine*. He was the recipient of the Beijing Outstanding Young Talent in 2016, IET Premium Award, and IEEE ComSoc Green Communications and Computing Technical Committee 2017 Best Paper Award.

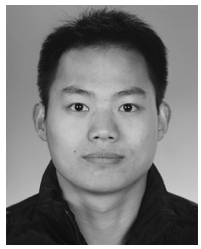

Fei Xiong is currently working towards the M.S. degree in communication engineering at North China Electric Power University, Beijing, China.

His research interests include green communications and smart grid.

Chen Xu (S'12–M'15) received the B.S. degree in communication engineering from the Beijing University of Posts and Telecommunications, Beijing, China, in 2010, and the Ph.D. degree from Peking University, Beijing, China, in 2015.

She is currently a Lecturer with the School of Electrical and Electronic Engineering, North China Electric Power University, Beijing, China. Her research interests mainly include wireless resource allocation and management, game theory, optimization theory, heterogeneous networks, and smart grid communication.

Dr. Xu is the recipient of the Best Paper Award in International Conference on Wireless Communications and Signal Processing (WCSP 2012), and the winner of IEEE Leonard G. Abraham Prize 2016.

Yejun He (SM'09) received the Ph.D. degree in information and communication engineering from the Huazhong University of Science and Technology, Wuhan, China, in 2005.

He is a Full Professor with the College of Information Engineering, Shenzhen University, China, where he is the Director of the Guangdong Engineering Research Center of Base Station Antennas and Propagation, Shenzhen University, China, and the Director of the Shenzhen Key Laboratory of Antennas and Propagation, Shenzhen University. His research interests include wireless mobile communication, antennas, and radio frequency.

Dr. He is a Fellow of IET.

Shahid Mumtaz (SM'16) received the M.Sc. degree in electrical engineering from the Blekinge Institute of Technology, Karlskrona, Sweden, and the Ph.D. degree in electrical and electronic engineering from the University of Aveiro, Portugal.

He is currently a Senior Research Engineer with the Institutõ de Telecomunicações, Aveiro, Portugal, where he is involved in EU funded projects. His research interests include MIMO techniques, multihop relaying communication, cooperative techniques, cognitive radios, game theory, energy efficient framework for 4G, position information-assisted communication, and joint PHY and MAC layer optimization in LTE standard.